UNIVERSITY of CALIFORNIA

SANTA CRUZ

**EFFECT OF BISMUTH DOPING ON THE MAGNETIC PROPERTIES
OF RARE-EARTH ORTHOFERRITES**

A thesis submitted in partial satisfaction of the
requirements for the degree of

BACHELOR OF SCIENCE

in

PHYSICS

by

Kelsey A. Collier

11 June 2010

The thesis of Kelsey A. Collier is approved by:

_____   _____
Professor Zack Schlesinger   Professor David P. Belanger
Advisor   Senior Theses Coordinator

_____
Professor David P. Belanger
Chair, Department of Physics

Abstract

Effect of Bismuth Doping on the Magnetic Properties of Rare-Earth Orthoferrites

by

Kelsey A. Collier

The purpose of this experiment was to investigate the magnetic properties of bismuth-doped rare-earth orthoferrites, prompted by scientific interest in and the possible device applications of multiferroics. The magnetic susceptibility of single-crystal samples of pure and bismuth-doped orthoferrites was measured as a function of temperature in a range from 2-300 K with an applied field of 1-5 T. Bismuth doping was found to modify the low-temperature interactions between the magnetic sublattices of some orthoferrites.

Contents

Acknowledgements

Zack Schlesinger, for offering me a wonderful opportunity, and making me think.

Art Ramirez, for teaching me about the subtleties of magnetization.

Andrew LaForge, for patiently explaining lab procedures and teaching practical skills.

Justin Bond and Jessica Missaghian, for all the work we shared between us.

My family, for always encouraging me to ask questions.

1 Introduction

Multiferroic compounds exhibit interesting properties, the exploration of which can expand our physical understanding of solid state phenomena, as well as suggesting a potential for device applications. A multiferroic material is one which exhibits at least two types of ferroic order in the same phase. These may be ferrotoroidicity, ferroelasticity, or, most commonly, ferroelectricity and some form of antiferromagnetism [1]. Most multiferroics are compounds that are both ferroelectric and ferrimagnetic within some temperature range.

These ferroic orders are properties that emerge from microscopic ordering. Specifically, a ferroelectric is a material with an electric dipole moment, often resulting from a displacement of ions in a uniform direction or a distortion of planes within the crystal structure. A ferromagnet is a material with a macroscopic magnetic moment resulting from an ordering of the magnetic moments generated by the spins of unpaired electrons, an ordering in which they all point in the same direction. An antiferromagnet is a material with no macroscopic magnetic moment which nonetheless has an intrinsic ordering of the unpaired spins. Neighboring spins orient opposite each other so as to cancel out their combined moment. A ferrimagnet is a material with a small macroscopic magnetic moment, resulting from an anitferromagnetic ordering of spins in which the combined moment is not entirely canceled out. This can occur because magnetic sublattices have moments of different magnitude or as a result of geometric frustration, such as a triangular lattice or canting (tilting) of sublattices [2].

Some multiferroic compounds exhibit a coupling between different types of ferroic order. This coupling is generally mediated by the lattice. A ferroic ordering causes a distortion of the lattice,

which in turn effects or even induces a different ferroic ordering. This coupling therefore indicates a system in which changes to one of the ferroic orders of the compound, perhaps as the result of an applied field, change the other ferroic order.

Why is there an interest in multiferroics? Compounds which exhibit strong magnetoelectric coupling hold intrinsic scientific interest and also have potential applications in the realization of electrically adressable magnetic memory and composite circuit devices. These devices would function by exploiting a coupling between the magnetization and polarization of a multiferroic compound. This would result in the application of a magnetic field changing the compound's response to an electric field, and vice versa. This applied magnetic field would change the dielectric susceptibility, just as an applied electric field would change the magnetic susceptibility. This would allow for magnetic memory to be read from a voltage, and for a composite circuit device coupling voltage and magnetic field.

There are several materials issues hindering the development of these applications. Current multiferroics are limited by the small magnitude of their electric and/or magnetic moments, the temperature range at which they exhibit multiferoic properties, or the weakness of the magnetoelectric coupling between the two orders. Realization of these applications requires a multiferroic with strong magnetic and electric moments, emerging above room temperature, with a strong coupling between the magnetic and electric orders. A better fundamental understanding of magnetic and lattice interactions is necessary to manipulate the coupling mechanism.

The crystals investigated in this work are derived from the $(R)FeO_3$ formula, where R is either a rare earth or bismuth ion. These materials crystallize in an orthorhombically distorted perovskite structure. The basic perovskite structure is shown in Fig. 1.1.
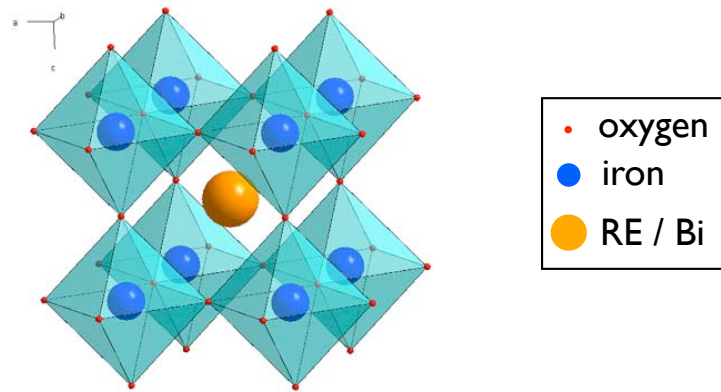
Figure 1.1: Basic perovskite structure. Image obtained from the website of the Cava group at Princeton: http://www.princeton.edu/ cavalab/tutorials/public/structures/perovskites.html.

Each iron ion is surrounded by an octahedral arrangement of six oxygen atoms; each oygen atom is shared between two octahedra. The bismuth or rare earth ion is surrounded by a cage of eight of the octahedral units. In orthoferrites and bismuth ferrite, the oxygen cages are distorted by a bending of the oxygen-iron-oxygen bonds in the vertical axis.

Why investigate bismuth-doped orthoferrites? The orthoferrites $DyFeO_3$ and $GdFeO_3$ have been shown to be multiferroics, exhibiting both ferroelectric and ferrimagnetic order at very low temperatures [3, 4]. When samples are cooled to low temperatures, the iron spins order antiferromagnetically. There are two magnetic sublattices of iron ions in orthoferrites; the spins on these lattices order opposite their neighbors, but the sublattices are canted–they are not directly parallel–so a ferrimagnetic moment emerges. The alignment of the spins causes attractive and repulsive forces between alternating layers of the materials, a phenomenon called exchange striction. This striction causes a distortion in the lattice structure, as planes bend together or apart. This distortion creates an overall dipole moment. This is the strong coupling we are looking for, the strongest kind possible: the ferroelectric order is directly induced by the ferrimagnetic order. This strong magnetoelectric coupling makes the orthoferrites an interesting series of compounds to research.

Another interesting multiferroic is $BiFeO_3$, a room-temperature multiferroic. It actully exhibits antiferromagnetic and ferroelectric ordering well above room temperature. The antiferromag-

netic ordering results from the alignment of the iron spins; the ferroelectric ordering results from the displacement of the bismuth ions away from the center of the oxygen cages. Unfortunately, the magnetoelectric coupling is very weak.

The orthoferrites $DyFeO_3$ and $GdFeO_3$ have the strong magnetoelectric coupling that is desired but are multiferroic only at very low temperature; $BiFeO_3$ is a room-temperature multiferroic but has very weak magnetoelectric coupling. It therefore seems interesting to investigate the magnetic and electric properties of bismuth-doped orthoferrites, to see if and how these properties may be combined.

Magnetization is a complex phenomenon in the orthoferrites, emerging from an interaction between two iron magnetic sublattices, a rare earth magnetic lattice (unless the rare earth element is nonmagnetic), and the lattice structure [5]. Below the Nèel temperature, the two iron magnetic sublattices orient antiferromagnetically. However, the distortion of the perovskite structure means that the two sublattices are not directly parallel; the canting of the sublattices creates an overall ferrimagnetic moment along the vertical (c) axis.
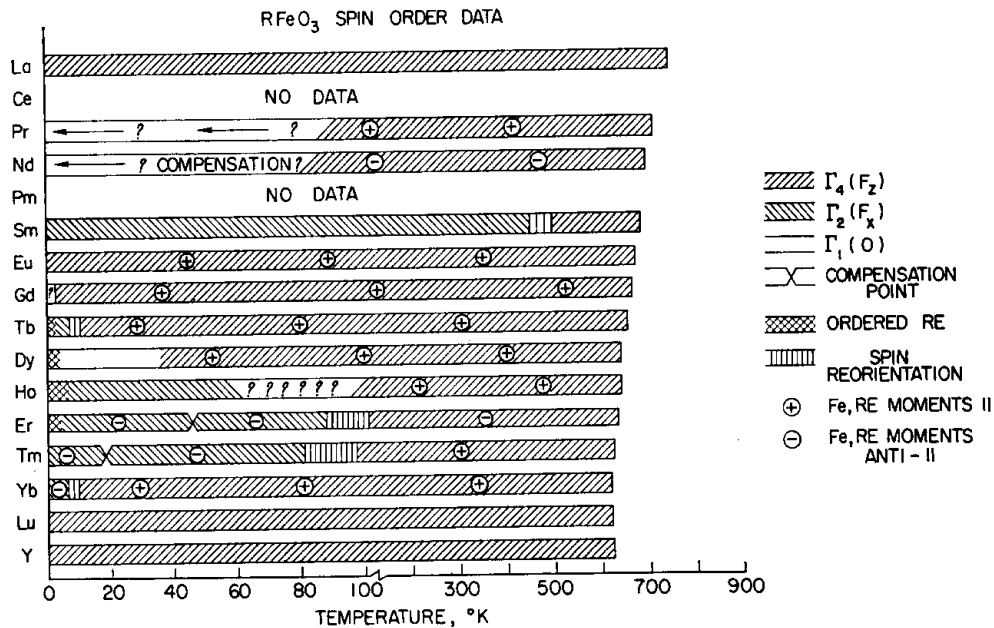

Figure 1.2: Magnetic ordering of rare-earth orthoferrites. This figure was taken from the White review of rare-earth orthoferrites.

As shown in the Fig. 1.2 above, further ordering occurs only if the rare earth ions have magnetic moments. The rare earth moments can then align with the exchange field between the iron magnetic sublattices. In some systems a spin-reorientation transition is observed; as one the system is cooled to about 50 K, the interaction between the magnetic moments of the rare-earth ions and the exchange field between the two iron sublattices can cause the ferrimagnetic moment of the iron moments to rotate from the vertical axis to the horizontal plane (a spin-reorientation transition). During this interaction the rare earth spins align either parallel or antiparallel to the exchange field between the two iron sublattices. If the rare earth spins align antiparallel to the iron moment, a compensation point can be seen where the moments cancel each other out. Finally, in the range of 1-4 K, the rare-earth spins order. A sampling of the range of behavior can be seen in the results section.

2 Experiment

The focus of this experiment was on how bismuth doping effects the magnetic ordering of orthoferrites. In the bismuth-doped orthoferrites, some percentage of the rare-earth ions were substituted for by bismuth ions when the crystals were grown. Therefore some percentage of the lattice sites normally occupied by the rare-earth ion are instead occupied by a bismuth ion.

The relative sizes of the ions ensures that the bismuth subsitutes for a rare-earth ion rather than an iron atom. According to the table of ionic radii compiled by Shannon and Prewitt [6], a Bi^{3+} ion in a crystal lattice with eight nearest neighbors has a radius of 1.25 Å. The rare earth ions range from Lu^{3+} , with a radius of 1.11 Å, to Sm^{3+}, with a radius of 1.23 Å. An Fe^{3+} ion with six nearest neighbors has a radius of 0.69Å.

The single-crystal samples examined were grown by J.P. Remeika at Bell Labs between 1965 and 1970. Given the technical limits at the time these samples were grown, the amount of bismuth content indicated on the sample cases is purely nominal. Recent x-ray diffraction measurements by Theo Siegrist at Florida State University indicated that the bismuth doping was generally in the range of 10%, although not all samples marked as doped contained bismuth. These measurements also allowed samples with orthoferrite structure to be separated from those with garnet and magnetoplumbite structure.

Magnetization measurements were made with a Quantum Design Magnetic Properties Measurement System (MPMS) [7], as shown in Fig. 2.1.
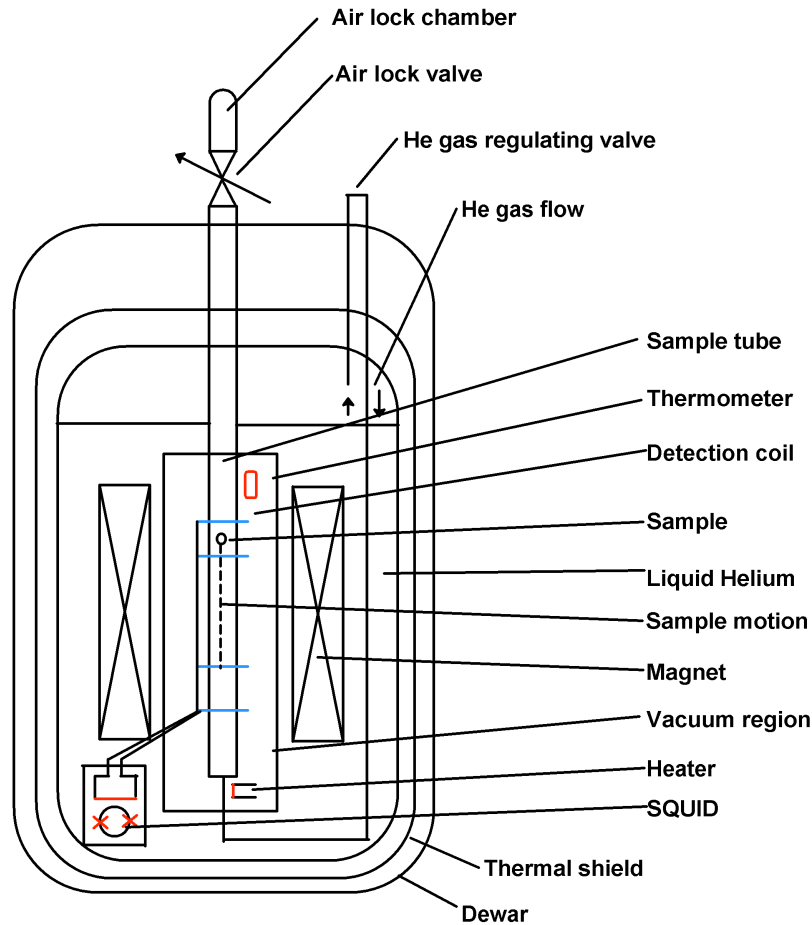
Air lock chamber

Air lock valve

He gas regulating valve

He gas flow

Sample tube

Thermometer

Detection coil

Sample

Liquid Helium

Sample motion

Magnet

Vacuum region

Heater

SQUID

Thermal shield

Dewar

Figure 2.1: Schematic diagram of Quantum Design MPMS unit. Image obtained from "Practical Guide to Using a SQUID". http://cnx.org/content/m22968/latest/

The MPMS unit consists of a large dewar with a central cylinder into which the sample is inserted. The cylinder is surrounded by a vacuum chamber. The chamber is immersed in a reservoir of liquid helium. A heater at the base of the vacuum chamber allows helium gas to be circulated through the chamber to cool the sample. Also submerged in the liquid helium reservoir is a superconducting coil, used to generate a magnetic field of up to five Tesla in the sample region.

Measurements of the magnetic moment of the sample are made by a Superconducting Quantum Interference Device (SQUID), surrounded by a superconducting magnetic shield within the reservoir. The SQUID is connected by superconducting wires to four small superconducting wire coils wound around the central cylinder. These coils are oriented such that the upper- and lowermost are

wound in one direction, the central two in the opposite direction. The SQUID, which contains a superconducting loop with two Josephson junctions, converts the current to a voltage when the sample is raised and lowered through these coils.

The Josephson junctions [8] are small nonsuperconducting regions, dividing the loop into two superconducting regions. Each of these regions is connected to a pair of the coils wrapped in the same direction. As the sample is moved vertically within the cylinder, the resulting magnetic flux induces a current within the coils. Because the pairs of coils are wound in opposite directions, the induced current will flow in opposite directions. The induced current within the two regions of the SQUID coil will therefore flow in opposite directions. On one side of the coil, the induced current will flow in the same direction as the intrinsic current. On the other side of the coil the induced current will flow against the intrinsic current. With a sufficiently large intrinsic current, tunneling of Cooper pairs through the junctions occur and the superconducting ring becomes resistive, with a voltage across it proportional to the magnetic flux. Because it is the voltage resulting from the difference in the two currents being measured, stray effects from nearby magnetic objects do not impact the measurement of the small magnetic moment of the sample.

The first stage of the experiment was to take a series of measurements of the magnetic properities of each of the orthoferrites, and compare the doped and undoped properties. For these measurements, cubic crystals were selected from the sample boxes. The crystal was weighed and then placed securely in half of a gel capsule, packed down with a small segment of a cotton ball. This capsule was placed into a generic plastic straw, and secured with fishing line and a sewing needle. The crystal was therefore kept from shifting during the magnetization measurements. The sample straw was then inserted into the MPMS system.

The next stage of the experiment involved taking anisotropic measurements–measuring magnetization along each of the three primary axes of the crystals. This enabled a more precise understanding of the transitions and reorientations suggested by the preliminary examination. The crystals selected were rectangular prisms with three obvious axes. Cylindrical sample mounts were prepared

by first hardening epoxy in a plastic straw mold. A segment of the expoxy was removed and a groove filed into it, based on the size and desired orientation of the sample crystal. The crystal was then placed into the groove with one of its three primary axes parallel to the straw (parallel to the applied magnetic field) and secured with nonmagnetic tape. The cylinder was then inserted into a straw and secured with fishing line. The sample straw was then inserted into the MPMS system.

Magnetization was measured as a function of temperature over a range of 2-300 K, with an applied field of 1000 Oe. The heater and helium gas were used to set the temperature of the sample chamber, and then two measurements of voltage as a function of vertical position were taken, as the sample was moved vertically through the coils. The pair of measurements was averaged, and the magnetic moment of the sample calculated as the integral of the voltage curve. The final output was therefore magnetization of the sample as a function of temperature.

3 Results

The basic measurement taken by the MPMS is of the voltage induced as the sample passes through the coils. A typical plot of voltage versus vertical displacement can be seen in Figure **??**. The sample begins below the coils. As it moves up through the lowest coil, a positive voltage is induced. As it moves up through the two center coils, the ones wound in the opposite direction, a strong negative voltage is induced. As it moves up through the top coil, another positive voltage is induced. The sample is then moved down through all of the coils, and the measurement repeated.
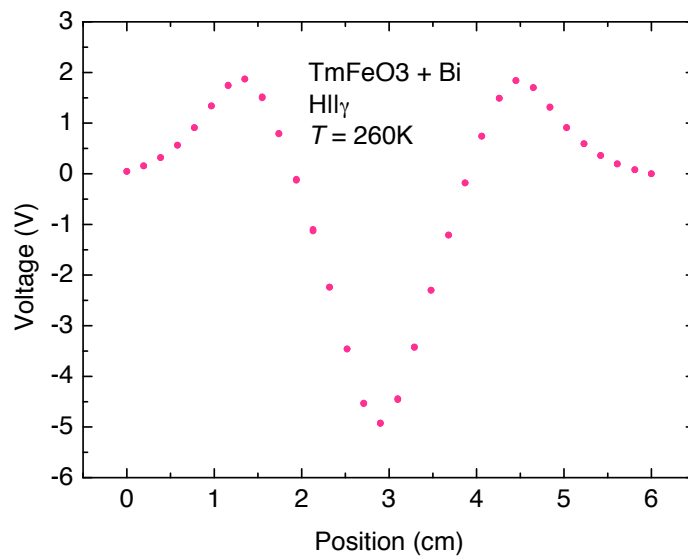
Figure 3.1: Voltage as a function of vertical displacement for $TmFeO_3+$ Bi.

This voltage is then used to calculate the magnetic moment of the sample. Data were then

exported from the MPMS system as a data table containing the magnitude of the applied magnetic field, the temperature of the sample, and the measured magnetic moment. A section of a data sheet is included as Table 3.1.

Field (Oe)	Temperature (K)	Long Moment (emu)
1000	10.0	0.119
1000	9.71	0.122
1000	9.40	0.124
1000	9.10	0.127
1000	8.80	0.130
1000	8.50	0.133
1000	8.20	0.136
1000	7.90	0.139
1000	7.60	0.142
1000	7.30	0.146
1000	7.00	0.149
1000	6.70	0.153
1000	6.40	0.157
1000	6.10	0.161
1000	5.80	0.165
1000	5.50	0.170
1000	5.20	0.175
1000	4.90	0.179
1000	4.63	0.182
1000	4.30	0.192
1000	4.01	0.192
1000	3.68	0.193
1000	3.40	0.194
1000	3.10	0.195
1000	2.80	0.197
1000	2.49	0.199
1000	2.20	0.202

Table 3.1: Example of MPMS output data for $GdFeO_3$ in the range of 10-2.2K

This output was then further processed to determine the magnetic susceptibility, as shown in Eq. 1:

$$\chi = \frac{M}{H} \Big/ \frac{m}{m_{\mathrm{mol}}}$$

where χ is the magnetic susceptibility, M is the magnetic moment, H the applied magnetic field, m the mass of the sample, and m_{mole} the molar mass of the orthoferrite.

The susceptibility was then plotted as a function of temperature. The plot from the data

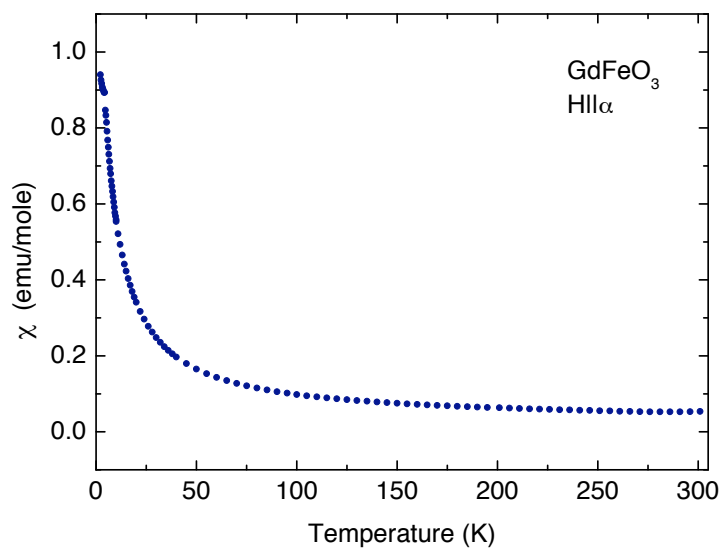referenced above is included as Fig. 3.2.

Figure 3.2: Magnetic susceptibility of GdFeO$_3$.

This is one set of data from an anisotropy study. The measurement was taken with the sample crystal aligned with its shortest axis parallel to the magnetic field.

4 Analysis

The initial measurements showed the range of magnetic behaviors seen in the orthoferrites, and indicated the general effects of bismuth doping. With anisotropic data the magnetic ordering along each axis, and any transitions between the axes, can be seen clearly. The subtleties of the interesting behavior suggested by the initial measurements are revealed by these more complete measurements.

For several of the orthoferrites investigated, including $SmFeO_3$, the bismuth doping had little effect on the magnetic susceptibility. For other orthoferrites, including $TmFeO_3$, $ErFeO_3$, and $HoFeO_3$, the bismuth doping modified the low-temperature interactions between the iron and rare-earth magnetic sublattices.

The $GdFeO_3$ compounds seem have a strong variation resulting from bismuth doping. The initial measurement of their magnetic susceptibilities is shown in Fig. 4.1.
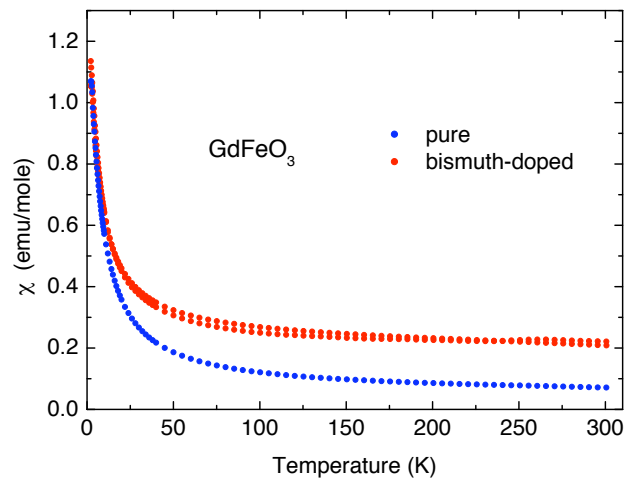
Figure 4.1: Magnetic susceptibilities of GdFeO$_3$ compounds. Blue indicates pure orthoferrite, red bismuth doped.

These compounds appear to show an increase in the magnitude of the ferrimagnetic moment of the iron sublattices as a result of the bismuth doping. They also show a paramagnetic alignment of the Gd spins at very low temperatures, in the sharp increase in their magnetic susceptibilities at low temperatures.

This ordering can be seen more clearly in the anisotropic measurements of the GdFeO$_3$ compounds included as Fig. 4.2.
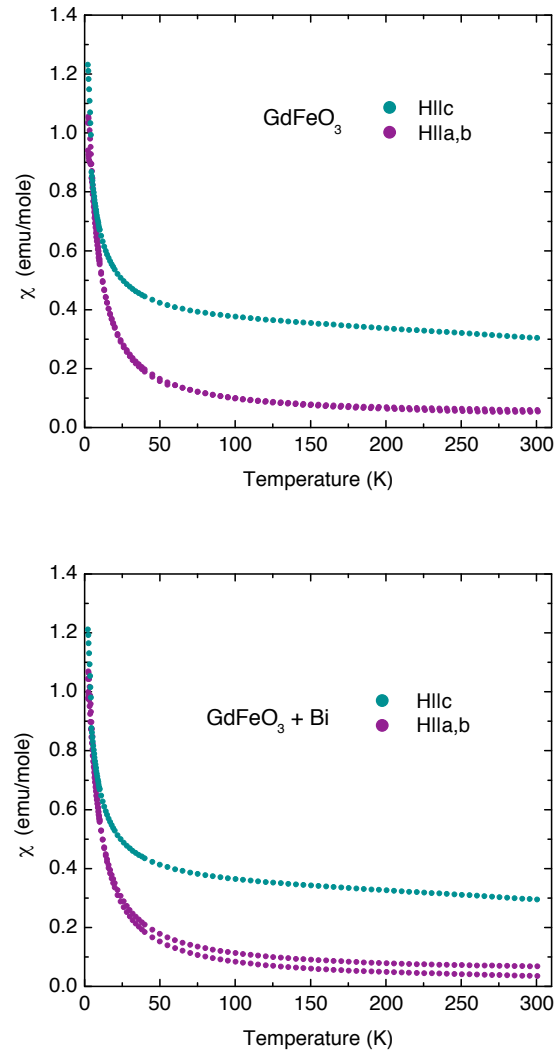
Figure 4.2: Anisotropic measurements of magnetic susceptibilities of GdFeO$_3$ compounds. Teal indicates the c axis, purple the a and b axes.

Examination of the anisotropic data shows that the Gd spins are aligning paramagnetically. They are not ordering along any one of the three axes, but rather aligning with the magnetic field as it is applied along each of the three axes. The ferrimagnetic moment of the iron spins shifts the magnetic susceptibility of the c axis to a higher value, but the same magnetic behavior is seen along each of the three axes. Examination of these data also suggests that the apparent increase in magnitude of the magnetic susceptibility as a result of the bismuth doping seen in the initial measurements is simply a

result of the chance alignment of samples along different axes during measurement.

The HoFeO$_3$ compounds exhibit an even wider range of behavior, although this is not immediately obvious. The initial measurements of the magnetic susceptibilities can be seen in Fig. 4.3.
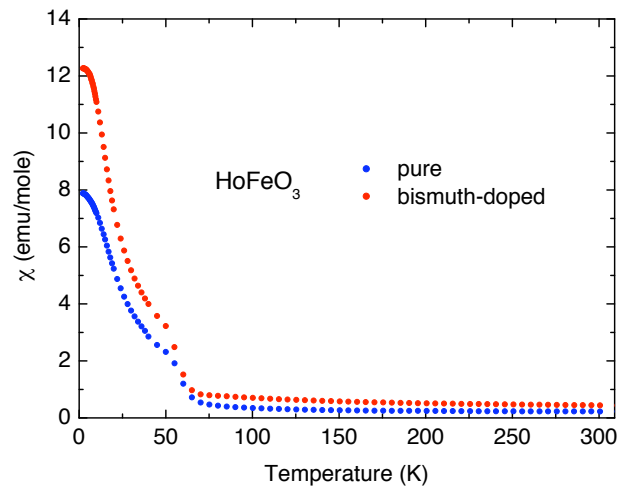

Figure 4.3: Magnetic susceptibilities of HoFeO$_3$ compounds. Blue indicates pure orthoferrite, red bismuth doped.

Unlike the previous compounds, there is no significant change in the magnitude of the ferrimagnetic iron moment resulting from the bismuth doping. There is, however, a noticeable effect on the low-temperature magnetic behavior. The bismuth doping apparently increases the magnitude of the magnetic moment resulting from the low-temperature interaction between the rare earth and iron sublattices.

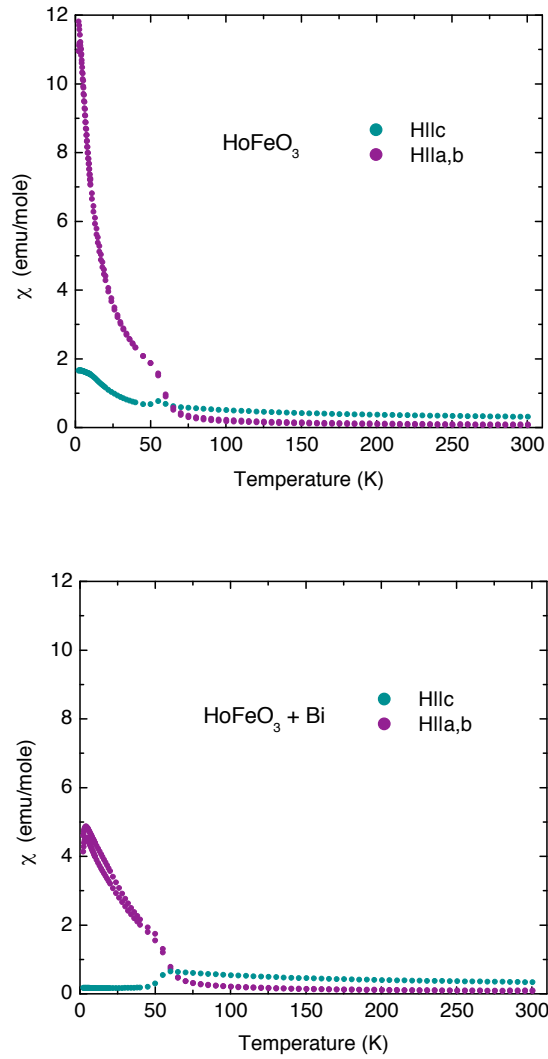This can be seen more clearly in the anisotropic measurements included in Fig. 4.4.

Figure 4.4: Anisotropic measurements of magnetic susceptibilities of $HoFeO_3$ compounds. Teal indicates the c axis, purple the a and b axes.

Examination of the anisotropic measurements shows that the pure samples in fact exhibit a significantly greater magnitude of the low-temperature magnetic susceptibility. This makes sense, since this susceptibility is a result of the ordering of the Ho spins. The Bi doping decreases the concentration of the Ho ions. The contrasting difference in magnitudes seen in the initial measurements most likely resulted from chance alignment of the samples along different axes.

These data also show a spin-reorientation transition at low temperatures. The magnetic

susceptibility along the c axis begins to decrease just above 50 K. At around the same temperature, the magnetic susceptibility along the other two axes begins to rise. This indicates the rotation of the ferrimagnetic moment of the iron spins from the c axis to the a-b plane, where it aligns with the ordering rare-earth ions. The increase in magnetic susceptibility along the c axis seen in the pure sample may indicate a sample that was slightly misaligned during measurement, so that some of the magnetization in the a-b plane was picked up. Comparison of the two plots also suggests that the doping shifted the ordering temperature slightly higher; in the bismuth-doped sample, the increase in magnitude corresponding to the rare-earth ordering can be seen to be a peak, which is beginning to drop off at the very low temperature edge. This peak is the temperature at which the rare-earth spins ordered. The pure sample shows a peak that is significantly larger in magnitude and both narrower and located at an even lower temperature.

The $ErFeO_3$ compounds exhibit a similarly complex range of behavior, as well as an anomalous sample. This can be seen in the initial measurements included in Fig. 4.5.
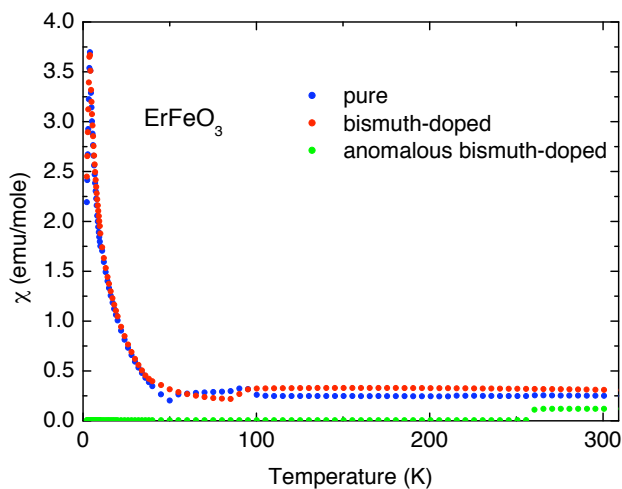

Figure 4.5: Magnetic susceptibilities of $ErFeO_3$ compounds. Blue indicates pure orthoferrite, red bismuth doped, green an anomalous behavior exhibited in a highly doped sample.

Both the pure and the bismuth-doped samples exhibit a ferromagnetic alignment at very low temperatures, causing a sharp peak in the magnetic susceptibilities. Interestingly, they exhibit small

compensation-like dips at different temperatures. The pure sample has a sharp dip around 50 K. The doped small has a wider dip around 80 K. The anomalous compound, a heavily doped sample, will be addressed later.

The variations in the low-temperature behavior of the compounds can be seen more clearly in the anisotropic measurements included in Fig. 4.6.
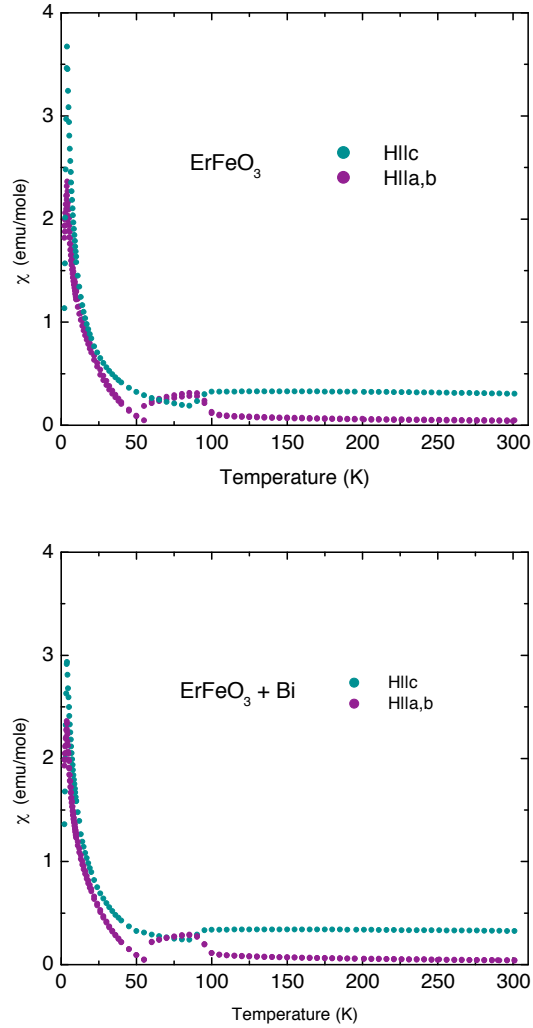

Figure 4.6: Anisotropic measurements of magnetic susceptibilities of ErFeO$_3$ compounds. Teal indicates the c axis, purple the a and b axes.

Again, the magnitude of the magnetic susceptibility resulting from the ordering of the rare-earth spins decreases with bismuth doping. Both samples exhibit a compensation-like dip in the

magnetic susceptibility along the c axis, but this dip is more pronounced in the pure sample. This dip apparently corresponds to a spin-reorientation transition, as there is a corresponding increase in the magnitude of the magnetic susceptibility in the a-b plane. Interestingly, the spins apparently rotate back to their previous alignment at the end of the transition.

The $TmFeO_3$ compounds also exhibit a complex range of behavior, including another anomalous sample. The initial measurements are included in Fig. 4.7.
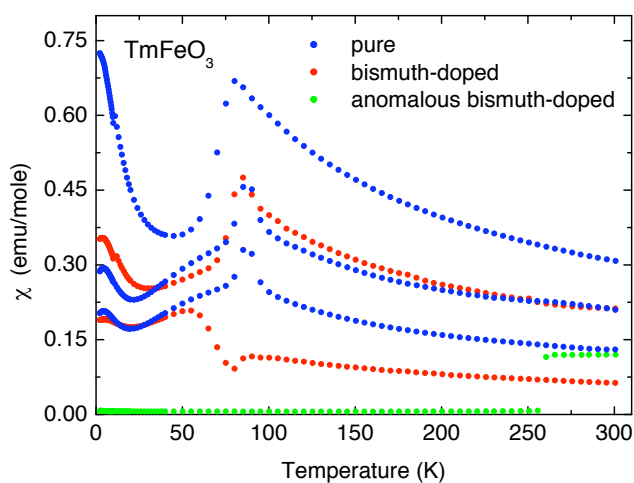

Figure 4.7: Magnetic susceptibilities of $TmFeO_3$ compounds. Blue indicates pure orthoferrite, red bismuth doped, green an anomalous behavior exhibited in a highly doped sample.

These data apparently show a significant difference between the pure and bismuth-doped samples. The pure samples exhibit a peak where the doped sample exhibits a dip. The marked bismuth-doped sample that exhibits the same peak as the pure samples was assumed to have, due to the difficulties of growing these crystals, have not actually picked up any bismuth. All of the samples, except for the anomalous one, show a paramagnetic alignment of the rare-earth spins at low temperatures.

Unfortunately, examination of the anisotropic measurements shows that the effects of the bismuth doping are not quite so dramatic. These measurements are included in Fig. 4.8.
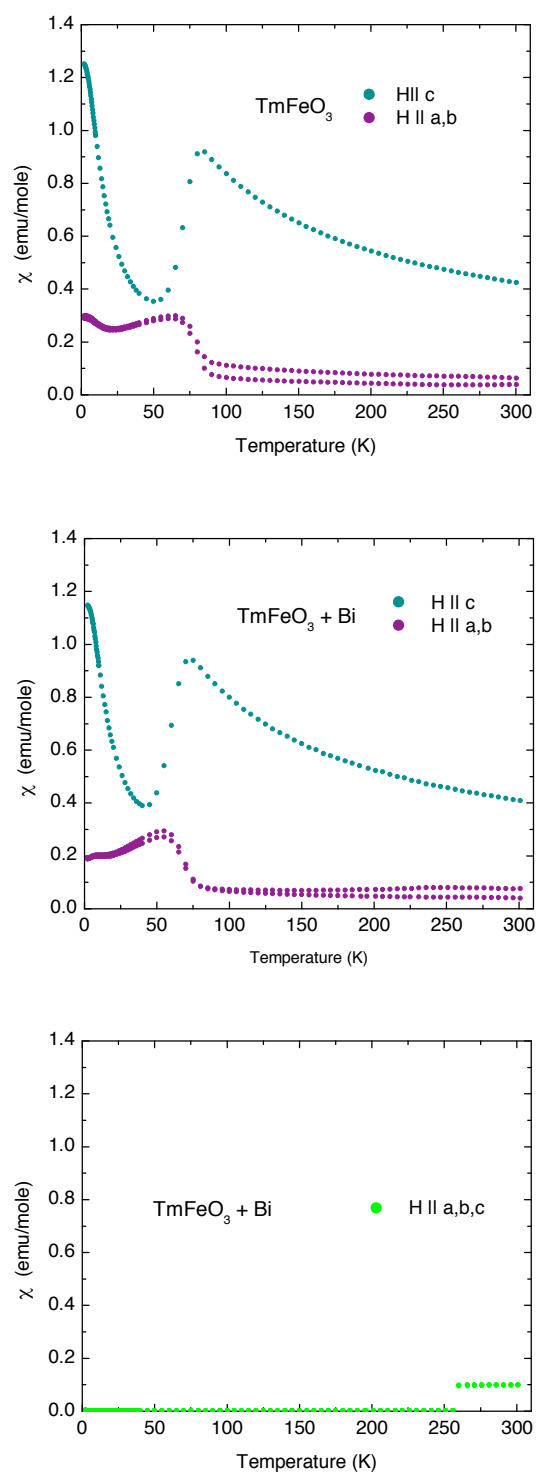
Figure 4.8: Anisotropic measurements of magnetic susceptibilities of TmFeO$_3$ compounds. Teal indicates the c axis, purple the a and b axes.

The dramatic difference in behavior is between the c axis and the a-b plane. These compounds show a strong spin-reorientation, as the magnetic susceptibility along the c axis drops and the susceptibility in the a-b plane rises. However, there are noticeable effects from the bismuth doping. The temperature of this transition is shifted down, and the magnitude of the magnetic susceptibility resulting from the paramagnetic alignment of the rare-earth spins at low temperature is suppressed.

The measurement done of the anomalous sample, again a highly doped sample, shows some interesting behavior. The magnetic susceptibility is the same along all three of the axes. The sample is weakly ferromagnetic at high temperatures, and has a very sharp antiferromagnetic transition around 260 K. An interesting transition occured in the measured voltage at that temperature range, as indicated in Fig. 4.9.
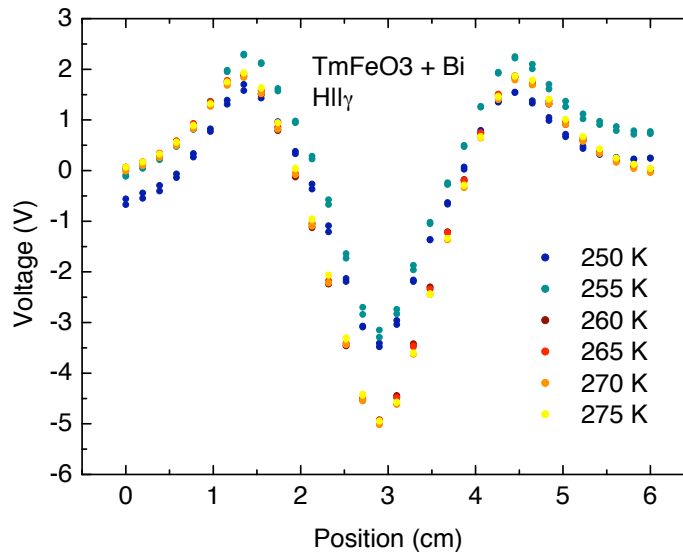

Figure 4.9: Voltage curves measured around the transition temperature of $TmFeO_3+$ Bi curve exhibiting anomalous behavior.

The voltage-position curves exhibit a distinct change in behavior at the transition temperature. The voltage is no longer going to zero when displacement of the sample is zero. All of these samples were marked as having high levels of bismuth doping. Interestingly, measurement with a multimeter also showed that these crystals have a finite resistance on the order of 1-10 MΩ at room

temperature, and so are not insulators like the rest of the orthoferrite samples.

5 Conclusions

The complexity of magnetic interactions in solids is seen in the varied ways in which bismuth doping affects the magnetic order of orthoferrites. In some cases, doping changed the low-temperature behavior resulting from the interaction between the iron magnetic sublattices and the rare earth magnetic lattice, or affected how the rare-earth spins ordered. Other members of my research group are investigating the phonon modes of the samples through spectroscopy. These phonon modes yield information about the electric ordering of the samples. By comparing these with the magnetic ordering revealed by the susceptibility measurements, it is possible to identify electromagnon modes–modes in which the electric and magnetic responses are coupled.

Bibliography

[1] Morkoc H, Izymskaya N, Alivov Ya. CRITICAL REVIEWS IN SOLID STATE AND MATE-RIALS SCIENCES. 34 89-172. 2009.

[2] Wolf W. Ferrimagnetism. REPORTS ON PROGRESS IN PHYSICS. 24 212-303. 1961.

[3] Tokunaga Y, Iguchi S, Arima T, Tokura Y. Magnetic-field-induced ferroelectric state in DyFeO3. PHYSICAL REVIEW LETTERS 101 9. AUG 29 2008.

[4] Tokunaga Y, Furukawa N, Sakai H, et al. Composite domain walls in a multiferroic perovskite ferrite. NATURE MATERIALS 8 7 558-562. JUL 2009.

[5] White R. Review of Recent Work on the Magnetic and Spectroscopic Properities of the Rare-Earth Orthoferrites. JOURNAL OF APPLIED PHYSICS. 40 3 1061-1069. March 1 1969.

[6] Shannon R, Prewitt C. Effective ionic radii in oxides and flourides. ACTA CRYSTAL. B25 925-946. 1969.

[7] McElfresh M. Fundamentals of magnetisim and magnetic measurements. Quantum Design 1994.

[8] Newrock R. What are Josephson junctions? How do they work?. SCIENTIFIC AMERICAN. November 24 1997.